AGU100 ADVANCING EARTH AND SPACE SCIENCE

Key Points:
- Calcareous nannofossil and stable isotope record from Northwest Atlantic Ocean spanning the early to middle Eocene
- The switch from warm-oligotrophic to temperate meso-eutrophic assemblages occurred in the aftermath of the Early Eocene Climatic Optimum
- Restoration of warmer condition during the early middle Eocene is associated with minor changes in calcareous nannofossil assemblages

Supporting Information:
- Supporting Information S1

Correspondence to:
C. Cappelli,
carlotta.cappelli@unipd.it

The Early to Middle Eocene Transition: An Integrated Calcareous Nannofossil and Stable Isotope Record From the Northwest Atlantic Ocean (Integrated Ocean Drilling Program Site U1410)

C. Cappelli[1] (ID), P. R. Bown[2], T. Westerhold[3] (ID), S. M. Bohaty[4] (ID), M. de Riu[1], V. Lobba[1], Y. Yamamoto[5] (ID), and C. Agnini[1,6] (ID)

[1]Dipartimento di Geoscienze, Università di Padova, Padova, Italy, [2]Department of Earth Sciences, University College London, London, UK, [3]MARUM – Center for Marine Environmental Sciences, University of Bremen, Bremen, Germany, [4]Ocean and Earth Science, National Oceanography Centre Southampton, University of Southampton, Southampton, UK, [5]Center for Advanced Marine Core Research, Kochi University, Kochi, Japan, [6]Department of Geological Sciences, Stockholm University, Stockholm, Sweden

Abstract The early to middle Eocene is marked by prominent changes in calcareous nannofossil assemblages coinciding both with long-term climate changes and modification of the North Atlantic deep ocean circulation. In order to assess the impact of Eocene climate change on surface water environmental conditions of the Northwest Atlantic, we developed calcareous nannoplankton assemblage data and bulk stable isotope records ($\delta^{18}O$ and $\delta^{13}C$) across an early to middle Eocene interval (~52–43 Ma) at Integrated Ocean Drilling Program Site U1410 (Southeast Newfoundland Ridge, ~41°N). At this site, early Eocene sediments are pelagic nannofossil chalk, whereas middle Eocene deposits occur as clay-rich drift sediments reflecting the progressive influence of northern-sourced deep currents. Between the end of Early Eocene Climatic Optimum (EECO) and the Ypresian/Lutetian boundary, calcareous nannofossils switched from an assemblage mainly composed of warm-water and oligotrophic taxa (*Zygrhablithus*, *Discoaster*, *Sphenolithus*, *Coccolithus*) to one dominated by the more temperate and eutrophic reticulofenestrids. The most prominent period of accelerated assemblage change occurred during a ~2-Myr phase of relatively high bulk $\delta^{18}O$ values possibly related to the post-EECO cooling. Although the dominance of reticulofenestrids persisted unvaried throughout the middle Eocene interval, early Lutetian (~47.4 to 47 Ma) stable isotope records indicate a reversal in the paleoenvironmetal trends suggesting a potential restoration of warmer conditions. Importantly, our data indicate that the ~2-Myr interval immediately following the EECO was crucial in establishing the modern calcareous nannofossil assemblage structure and also reveal that the establishment of *Reticulofenestra*-dominated assemblage occurred prior to the onset of persistent deep current system in the Northwest Atlantic.

1. Introduction

Through the early and middle Eocene, the global climate system shifted from the warmest global temperatures of the last 65 Myr to a long phase of global cooling that culminated in the Early Oligocene Glacial Maximum (e.g., Coxall & Pearson, 2007). The climate phase known as the Early Eocene Climatic Optimum (EECO) was an interval (~53–49 Ma) of extreme warmth characterized by low oxygen stable isotope values (Bijl et al., 2009; Hollis et al., 2009, 2012; Westerhold et al., 2018; Zachos et al., 2001, 2008), very high levels of atmospheric pCO_2 (Beerling & Royer, 2011; Pagani et al., 2005; Zachos et al., 2008), and subdued equator-to-pole temperature gradients (Bijl et al., 2009; Cramwinckel et al., 2018; Greenwood & Wing, 1995). This prolonged interval of warmth was further punctuated by numerous events of rapid warming (hyperthermals), which are recorded as transient carbon isotope excursions (CIEs), related to massive releases of ^{13}C-depleted carbon in the ocean-atmosphere system. Hyperthermals are also associated with dissolution of deep-marine carbonates and negative oxygen isotope excursions, indicative of ocean chemistry buffering and rapid global warming (Cramer et al., 2003; Dickens, 2011; Kirtland Turner et al., 2014; Sexton et al., 2011). Although hyperthermals are typical of the middle Paleocene to early Eocene interval, the EECO represents their climax in terms of frequency and magnitude (Lunt et al., 2011). The demise of the extremely warm conditions following the EECO coincides with the onset of deep ocean and global

cooling, but hyperthermal perturbations in the carbon cycle persisted into the middle Eocene, for example, as shown by the Middle Eocene Climatic Optimum (MECO, Bohaty & Zachos, 2003; Bohaty et al., 2009). Eventually, long-term Eocene cooling crossed a climatic threshold at the Eocene-Oligocene Transition (EOT), when the growth of permanent ice sheets took place on Antarctica (Coxall & Pearson, 2007). Variations in ocean paleocirculation related to the tectonic evolution of the Southern Ocean (Bijl et al., 2013; Kennett, 1977) as well as declining greenhouse gas concentrations (Anagnostou et al., 2016; Cramwinckel et al., 2018; Pagani et al., 2005) are suggested as the primary drivers for global cooling during the Eocene.

In this study, we use calcareous nannoplankton to investigate the relationship between Eocene changes in the geosphere and the evolution of the biosphere because these phytoplankton are sensitive to environmental change and lie at the base of the ocean food chain. Any change observed in calcareous nannoplankton can thus be related to global paleoceanographic modifications and may result in changes at higher levels in the food web. Reconstructing the evolutionary history of this important marine calcareous phytoplankton group allows us to test how plankton evolution and climate interact. The late early to middle Eocene, in particular, is a relatively understudied time interval that includes the final early Eocene hyperthermal events and relatively stable early Lutetian interval (~52–43 Ma), providing the opportunity to observe evolutionary patterns during extreme climate phases as well as through more stable background conditions.

The EECO was an important time of evolutionary change in calcareous nannoplankton. In particular, the assemblages shifted permanently in character as the Paleocene Prinsiaceae family declined to extinction to be replaced by the extant reticulofenestrids (i.e., Noelaerhabdaceae family), which first appeared and rapidly expanded through this interval (Agnini et al., 2006; Schneider et al., 2011). The rise of this new group was accompanied by an increase in nannofossil diversity, which reached maximum levels in the middle Eocene (Bown et al., 2008).
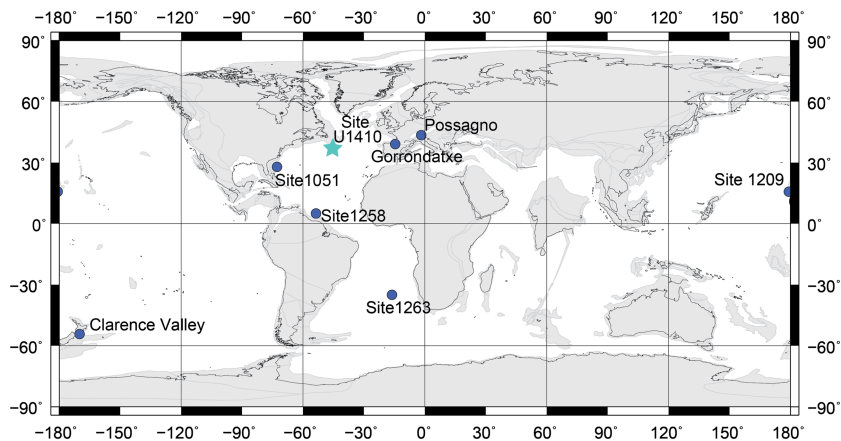
It is still uncertain whether environmental change during and shortly after the EECO was directly responsible for these changes in calcareous nannoplankton communities. Numerous lines of evidence support the idea that transient paleoclimate events through the Eocene (PETM, MECO, EOT) have induced both permanent and temporary modifications in nannofossil assemblages (e.g., Agnini et al., 2007; Bralower, 2002; Dunkley Jones et al., 2008; Gibbs et al., 2006; Toffanin et al., 2011; Villa et al., 2008). Schneider et al. (2011) suggest that the remarkable turnover between Prinsiaceae and reticulofenestrids during the EECO was related to a collapse in water column stratification, which resulted in a decline in the efficiency of the biological pump, with a minimum reached at ca. 51 Ma. Although the early to middle Eocene witnesses one of the most profound change in calcareous nannofossil assemblage, few studies (e.g., Schneider et al., 2011; Shamrock & Watkins, 2012) have documented nannofossil assemblage changes in detail across this time interval. This is mainly due to the scarcity of well-preserved, continuous, and expanded early to middle Eocene successions, with deep-sea sites in the North Atlantic Ocean typically characterized by chert horizons in the lower Eocene and condensed sequences or hiatuses across the early-middle Eocene transition (Erbacher et al., 2004; Muttoni & Kent, 2007; Norris et al., 2001; Norris et al., 2001).

Here we present a geochemical (bulk δ^{13}C, bulk δ^{18}O, and $CaCO_3$ content) and nannoplankton record from the North Atlantic Integrated Ocean Drilling Program (IODP) Site U1410 (Southeast Newfoundland Ridge) spanning from the final phase of the EECO to the lower middle Eocene (supporting information Figure S1; ~52–43 Ma). This site represents one of the most well-preserved and continuous deep-sea records of the early-middle Eocene transition (Norris et al., 2014) and is thus ideal (1) to document primary and secondary biostratigraphic biohorizons using quantitative data; (2) to analyze assemblage data in order to investigate changes in plankton communities over long and short time scales; (3) to document nannofossil and geochemical proxies (stable oxygen and carbonate data from bulk sediments) of paleotemperature, paleoproductivity, and other environmental parameters; and (4) to investigate links between biotic and environmental/climate change across the early to middle Eocene transition.

2. Materials and Methods

2.1. IODP Site U1410

Site U1410 (41°19.6993′N, 49°10.1847′W) was drilled during IODP Expedition 342 on the Southeast Newfoundland Ridge, offshore Newfoundland, in the Northwest Atlantic Ocean (Figure 1). Today, the

Figure 1. Location map at 50 Ma showing the position of IODP Site U1410 (solid green star). The locations of key sites documenting the early-middle Eocene transition are also reported (solid blue circles): Gorrondatxe section (Spain, Global Stratigraphic Section and Point for the base of Lutetian, Molina et al., 2011); the Possagno section (NE Italy, Agnini et al., 2006, 2014); ODP Site 1051 (Blake Nose, Agnini et al., 2014); ODP Site 1258 (Demerara Rise, Sexton et al., 2011; Westerhold et al., 2017, 2018); ODP Site 1209 (Shatsky Rise, Westerhold et al., 2018); ODP Site 1263 (Walvis Ridge, Westerhold et al., 2017, 2018); and Clarence valley (New Zealand, Slotnick et al., 2012, Slotnick, Lauretano, et al., 2015). Base map is available online (http://www.odsn.de/odsn/services/paleomap/paleomap.html).

oceanography of this area is strongly influenced by the presence of the warm Gulf Stream and the modern Deep Western Boundary Current, which is the primary southward-flowing component of the deep current system along the western North Atlantic Ocean basin. Site U1410 is currently positioned at a water depth of ~3,400 m, and it is estimated to have been at ~2,950 m at 50 Ma (Norris et al., 2014). At this site, a composite sedimentary succession was generated from drilling three holes, spanning the early Eocene to Pleistocene (Norris et al., 2012; Norris et al., 2014).

The study interval encompasses a transition from lower Eocene white to pinkish-white nannofossil chalk (Lithologic Unit IV) to middle Eocene greenish nannofossil clay (Lithologic Unit III; Norris et al., 2014). This prominent lithologic change likely reflects the onset of a drift sedimentation regime at ~47 Ma, as indicated by the increase of terrigenous clay-rich components at Site U1410 (Boyle et al., 2017) but also by erosional unconformities elsewhere. Significant changes in sedimentation rates are recorded at Site U1410, averaging ~0.6 cm/Kyr in the lower Eocene, typical of truly pelagic environments, to ~1.3–2.6 cm/Kyr in the middle Eocene (Norris et al., 2014). Higher sedimentation rates in the middle Eocene are interpreted to coincide with the onset of contourite drift deposition (Boyle et al., 2017). This new deep current system, fed by Northern Component Water, has been interpreted as the predecessor/progenitor of North Atlantic Deep Water (Coxall et al., 2018; Vahlenkamp et al., 2018).

2.2. Calcareous Nannofossil Assemblage Data

Calcareous nannofossil analysis was carried out on 207 samples spanning a ~156-m-thick interval. Smear slides were prepared from raw sediment samples using standard techniques (Bown & Young, 1998) and then investigated in light microscope at a magnification of 1,250×. The taxonomic concepts follow Aubry (1984, 1989), Perch-Nielsen (1985), Bown (2005), Bown and Dunkley Jones (2006, 2012), and Bown and Newsam et al. (2017), except for *Dictyococcites* and *Reticulofenestra* for which we follow Agnini et al. (2014). A minimum of 300 specimens per slide were counted for calcareous nannofossil assemblage data.

Principal component analysis (PCA) was performed in order to evaluate the main factors affecting variations in assemblage composition. The PCA was carried out on counts of the most abundant calcareous nannofossil genera using the free statistical software PAST (PAleontological STatistic; Hammer et al., 2011). For this analysis, we considered the following 17 groups: *Blackites*, *Campylosphaera*, *Chiasmolithus*, *Clausicoccus*, *Coccolithus*, *Cyclicargolithus*, *Dictyococcites*, *Discoaster*, *Ericsonia* (= *Coccolithus formosus*, auctorum), *Girgisia*, *Helicosphaera*, *Pontosphaera*, *Reticulofenestra*, *Sphenolithus*, *Toweius*, *Zygrhablithus*, and "others" that includes genera with abundance that never exceeds 1%.

2.3. PaleoEnvironmental Index

We developed a nannofossil-based PaleoEnvironmental Index (PEI) applicable to the early and middle Eocene based on the fluctuations of selected paleoecologically sensitive taxa, for which environmental preferences are relatively well established (Table 1). Temperate water and/or mesotrophic favoring taxa include *Reticulofenestra* and *Toweius* (Gibbs et al., 2006; Haq & Lohmann, 1976; Monechi et al., 2000; Persico & Villa, 2004; Villa et al., 2008, 2014), and warm-water and/or oligotrophic taxa include *Ericsonia*, *Coccolithus pelagicus*, *Discoaster*, *Sphenolithus*, and *Zygrhablithus* (Agnini et al., 2007; Bralower, 2002; Gibbs et al., 2006; Haq & Lohmann, 1976; Monechi et al., 2000; Villa et al., 2014; Wei & Wise, 1990). Based on the abundances of these two groups, we have calculated a PEI (e.g., Villa et al., 2008), which is defined as % temperate-mesotrophic group/ (% temperate-mesotrophic group + % warm-oligotrophic group). The relative abundance of the taxa with a designated paleoecological affiliation included in the PEI accounts for ~87% of total assemblages throughout the study interval. The relative abundance of taxa with uncertain ecological affinity, which never exceeds ~23%, is not used to calculate this index.

2.4. Geochemical Data

A total of 329 samples were powdered and analyzed for bulk sediment stable isotope composition and calcium carbonate content ($CaCO_3$). The analyses were carried out in the Stable Isotope Laboratory of the Department of Geosciences at the University of Padova using a Delta V Advance Isotopic Ratio Mass Spectrometer equipped with a Gas Bench II device. A known mass of sample (0.25–0.75 mg) was placed into headspace vials and flushed with helium. Each sample was treated with 10 ml of 100% phosphoric acid (EMSURE ® ≥99%) at 70 °C for approximately 3 hr and reacted with orthophosphoric acid at 70 °C. Isotopic values are reported in standard delta notation relative to the Vienna Pee Dee Belemnite (VPDB). An internal standard (white Carrara marble Maq 1: $\delta^{13}C$ = 2.58‰; $\delta^{18}O$ = −1.15‰ VPDB) periodically calibrated to NBS-19 IAEA reference material (Coplen et al., 2006) was used to normalize raw $\delta^{13}C$ and $\delta^{18}O$ values. A third internal standard (marble Gr1: $\delta^{13}C$ = 0.68‰; $\delta^{18}O$ = −10.44‰ VPDB) was run for quality assurance and repeated with precisions better than 0.07‰ for $\delta^{13}C$ and better than 0.09‰ for $\delta^{18}O$. The calcium carbonate content of each sample was calculated based on the beam height obtained during isotope mass spectrometer analysis (Spofforth et al., 2010). The beam height depends on the pressure of CO_2 liberated from the sample, which in turn is a function of the carbonate content of the sample. Apart from the Maq1 samples used to calibrate each sequence, every run contained at least 10 samples of Maq1 (weights range from 50 to 500 mg) distributed along the run. These standard samples serve to construct a linear fit line based on the beam height/standard weight ratio (with a r^2 always >0.99) that is used to calculate the carbonate content of the analyzed samples.

2.5. Age Model

2.5.1. Revision of Composite Records for U1408 and U1410

A composite record for Site U1410 was assembled during shipboard work for Holes U1410A, U1410B, and U1410C (Norris et al., 2014) and revised based on onshore-acquired XRF core scanning data (Boulila et al., 2018; Vahlenkamp et al., 2018). Despite the revision, calcareous nannofossil datums point to major condensed intervals that were not taken into account previously. Therefore, we reinvestigated the splices using the software tool Code for Ocean Drilling Data (Wilkens et al., 2017) allowing us to plot multiple data sets, including nannofossil biostratigraphy along high-resolution core images (Drury et al., 2018). The results and detailed discussion of splice revision can be found in the supporting information. Our revision is not limited to Site U1410 (Boulila et al., 2018) but also includes Site U1408 (Hull et al., 2017) because only both sites taken together reveal substantial discrepancies and misalignments in the previously published composite records. At Site U1410, our splice revision documents a doubling of cycles leading to serious cycle misidentification in Boulila et al. (2018; see the supporting information for details). Site-to-site correlation between U1408 and U1410 clearly documents major gaps, condensed intervals present and slumping. To this end, it is not possible to construct a reliable composite record for both sites in Chron C20r. Reinterpretation of calcareous nannofossil datum positions with respect to the revised splice suggests that the dominant cycles in the sediment are very likely precession related instead to obliquity as proposed by Boulila et al. (2018). The site-to-site correlation points to major issues in Chron 19r around the Late Lutetian Thermal Maximum event suggesting that even integrating U1408 with U1410 will not result in a complete stratigraphic record for Chron C21 to C18.

Table 1
Summary of Paleoecological Affinities as Suggested by Different Authors for Selected Taxa Used in the PEI

Author Taxon	Wei and Wise (1990)	Aubry (1992, 1998)	Monechi et al. (2000)	Bralower (2002)	Tremolada and Bralower (2004)	Persico and Villa (2004)	Gibbs et al. (2006)	Villa et al. (2008)	Schneider et al. (2011)	Villa et al. (2014)	This work
Ericsonia formosa	Warm		Warm-water	Warm/oligo-trophic	Warm/oligo-trophic			Warm/oligo-trophic	Warm/oligotrophic	Warm	Warm-water/oligo-trophic
Coccolithus pelagicus	Warm					Temperate		Temperate	Ubiquitous, higher abundance in the warm early Eocene	Temperate/eutrophic	Warm-water/oligo-trophic
Discoaster spp.	Warm	Oligotrophic	Oligotrophic	Warm/oligo-trophic	Warm/oligo-trophic		Oligotrophic	Warm/oligo-trophic	Warm/oligotrophic	Warm/oligo-trophic	Warm-water/oligo-trophic
Sphenolithus spp.	Warm		Warm (*S. moriformis*)	Warm/oligo-trophic			Oligotrophic	Warm/oligo-trophic	Warm/oligotrophic	Warm/oligo-trophic	Warm-water/oligo-trophic
Zygrhablithus spp.		Oligotrophic	Nearshore taxa	Warm/oligo-trophic	Relatively cool/meso-trophic			Temperate/eutrophic	No straightforward	Warm-water/oligo-trophic	Warm-water/oligo-trophic
Reticulofenestra spp.	Cool (*R. davi-esii*)		Cool			Temperate-cool		Mesotrophic	Cooler water/mesotrophic	Temperate and cool, eutrophic	Temperate water/meso-trophic
Toweius				Mesotrophic, wide tolerant	Cool/eutrophic				Cool/mesotrophic	Temperate water/meso-trophic	

All depths for samples and data in this study are given for the revised splice established here in a "corrected revised meter composite depth" (crmcd) scale, including an update to the magnetostratigraphy first published by Yamamoto et al. (2018). See Tables S1–S8 and Figures S2–S19. Ages are given following the Geological Time Scale calibration (GTS12, Vandenberghe et al., 2012). Tie points used are Chron boundaries (i.e., C21n/C20r; C20r/C20n) and the Top of the calcareous nannofossil *Tribrachiatus orthostylus* (50.49 Ma, Agnini et al., 2014 converted to GTS12).

2.5.2. Calcareous Nannofossil Biostratigraphy

The abundance of selected nannofossil index species was determined by counting the number of specimens in a predetermined area of the slide, usually 1 mm^2 (Agnini et al., 2014; Backman & Shackleton, 1983), but extended to 2 mm^2 (normalized to 1 mm^2) for rare index taxa (e.g., *Nannotetrina*, *Coccolithus gigas*, and *Reticulofenestra umbilicus*). Biohorizons were determined based on abundance patterns of index species and termed Base (B) and Top (T) for the stratigraphic lowest and highest occurrences of taxa. The Base of continuous and common (Bc) and Top of continuous and common (Tc) occurrences were used to define the first/last continuous presence of a specific taxon when it is preceded/succeeded by an interval of sporadic occurrences (Agnini et al., 2014; Backman et al., 2012). The biostratigraphic schemes adopted are those of Martini (1971), Okada and Bukry (1980), and Agnini et al. (2014). These quantitative, highly resolved data sets allow for the analysis of biostratigraphic reliability (e.g., Agnini et al., 2017; Raffi, 1999). This is particularly relevant for the lower and middle Eocene intervals, where numerous marker species have been found to be rare or even absent in some depositional settings or show sporadic abundance patterns around their level of evolutionary emergence and/or extinction. A comprehensive discussion of the selected biohorizons and comparison with previuos works (e.g., Agnini et al., 2016; Applegate & Wise, 1987; Backman, 1986; Backman & Hermelin, 1986; Berggren & Aubry, 1984; Bernaola et al., 2006; Bukry, 1973; Dallanave et al., 2009; Martini & Müller, 1986; Self-Trail et al., 2017; Wei and Wise, 1989) are provided in the supporting information and serve to strengthen our age model (see Text S1, Figure S20, and Table S1). Microphotographs of calcareous nannofossils are presented in Plates S1 to S12.

3. Results

3.1. Calcareous Nannofossil Assemblage Data

The calcareous nannofossil assemblages at Site U1410 are abundant and diverse. Preservation varies from moderate to good and is closely related to lithology. Calcareous nannofossils are moderately to well preserved in the lower Eocene nannofossil chalks, where they are typically affected by overgrowth, especially *Discoaster* and *Zygrhablithus*. Preservation is generally good to excellent in the overlying clay-rich drift sediments. This exceptional preservation is a distinctive feature of the Expedition 342 sites (Bown & Newsam, 2017) and allows for the preservation of very delicate structures (e.g., central area nets in *Reticulofenestra*), high abundances of small placoliths (mainly reticulofenestrids), and taxa that are highly susceptible to fragmentation (e.g., *Blackites*).

Nannofossil assemblages from Site U1410 display several general trends and prominent changes in their composition (Figure 2).
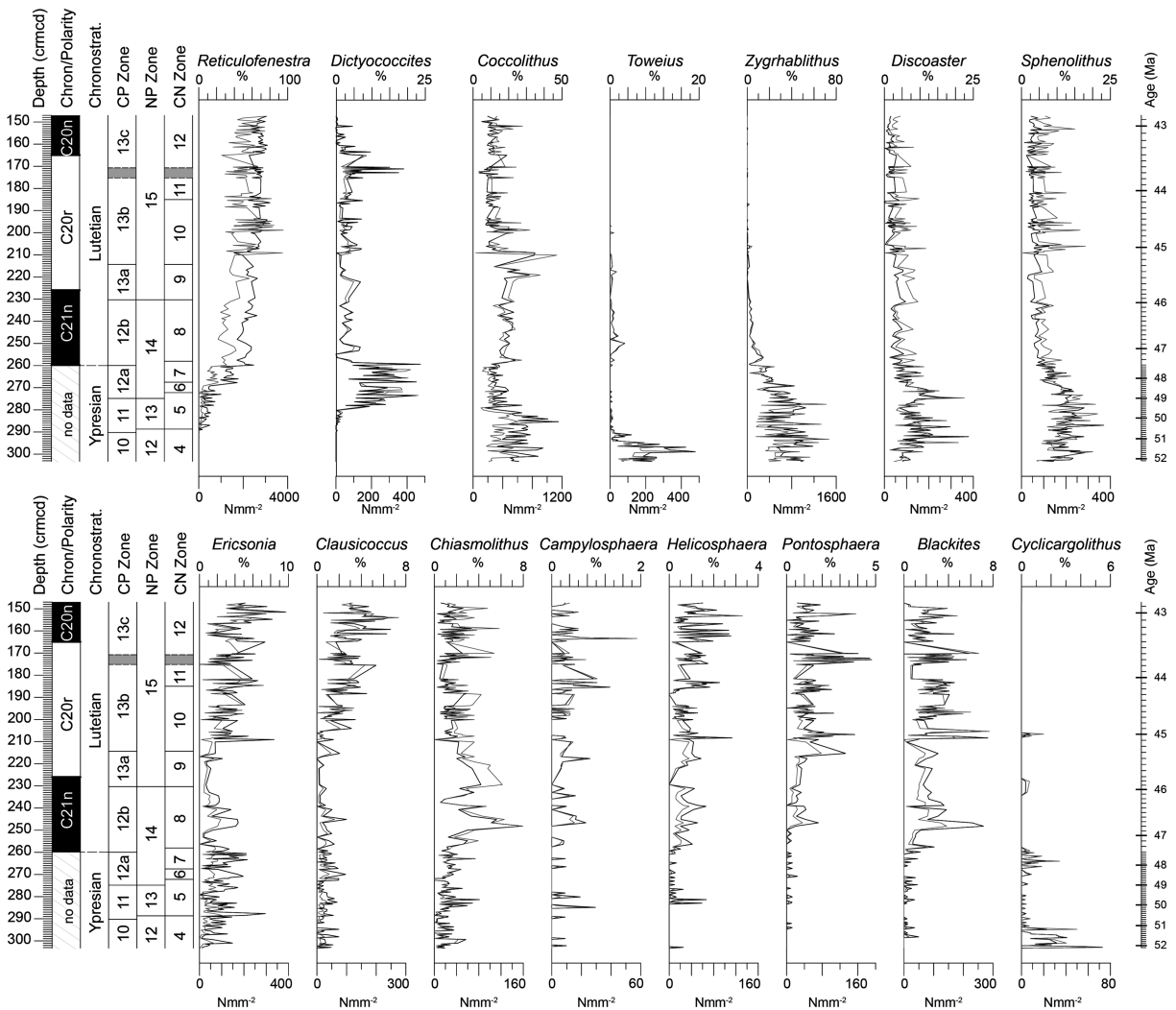
Reticulofenestra significantly increases in abundance from ~8% in the lower part of its range to ~50% above 260.77 crmcd and remains at this level in the upper part of the study interval.

Dictyococcites first appears at 286.74 crmcd but rapidly increases in abundance (from less than 1% to 11%) at 279.83 crmcd with high values (~12% on average) maintained up to 216.58 crmcd. At the top of the Ypresian (~258.92 crmcd), *Dictyococcites* drops and remains relatively constant at around 2%.

Toweius is consistently present from the base of the study interval up to 293.46 crmcd. It is common in the lower part of the study interval, peaking in abundance (~16%) between 290.55 and 288 crmcd. Above this level, *Toweius* progressively decreases to values <1%.

Coccolithus displays an average abundance of ~16%, with higher values (~26%) recorded before the expansion of *Reticulofenestra* between 303.29 and 274.44 crmcd.

Discoaster represents ~8% of the assemblages through the lower Eocene, with a peak of ~13% during the turnover between *Toweius* and *reticulofenestrids* (292.88–297.32 crmcd). A second peak in abundance (~11%) occurs in the upper part of the lower Eocene (between 277.10 and 269.57 crmcd). *Discoaster* shows

Figure 2. Relative (%, black line) and semiquantitative (N/mm², gray line) abundances of selected calcareous nannofossil genera from IODP Site U1410 are plotted against chronostratigraphy and calcareous nannofossil biostratigraphy: CP Zone (Okada & Bukry, 1980), NP Zone (Martini, 1971), and CNE Zone (Agnini et al., 2014). Magnetostratigraphy is taken from Yamamoto et al. (2018) converted to the new splice depth. The time scale to the right is calibrated to GTS12, and it is based on available chron boundaries and on the top of *Tribrachiatus orthostylus*.

an overall decrease in abundance above the early-middle Eocene transition, with values never exceeding 2% of the assemblages in middle Eocene samples.

Sphenolithus is relatively common (on average ~7%) reaching values around 12% in the lower Eocene but progressively decreases in the middle Eocene to ~4%.

Zygrhablithus is characterized by highly variable abundance through the study section. This genus is common in the lower Eocene (~33%) but dramatically declines above 268.45 crmcd. In middle Eocene samples, the abundance of this genus is generally ~1%.

Cyclicargolithus is a minor component of the assemblages. Higher abundances (up to ~5%) are recorded at the base of the study interval (~302 crmcd) and are mainly composed of *Cyclicargolithus luminis*.

Ericsonia (= *C. formosus*) and *Clausicoccus* are present from the base of the study section and occur throughout but are minor components of the assemblages (~3% and ~2%, respectively). They display a slight increase from ~200 crmcd upward.

Chiasmolithus is rare throughout but shows a slight increase in average abundance from ~1% to ~4% that is recorded between 250.92 and 238.19 crmcd.

Table 2
Summary of the PCA Results in Terms of Eigenvalue and % Variance

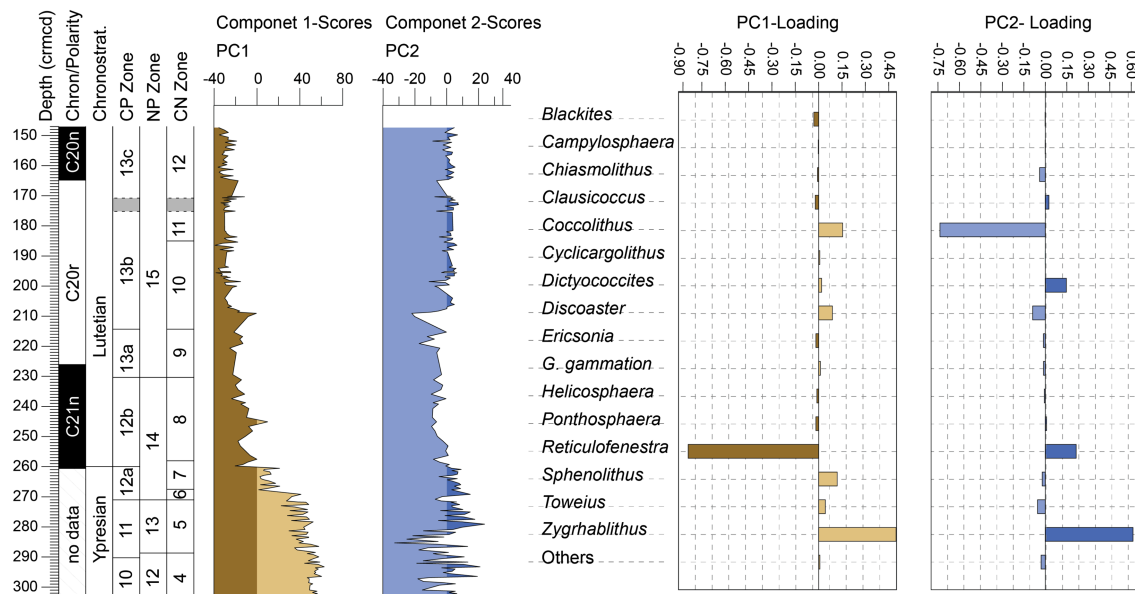| PC	Eigenvalue	% variance
1	1,117.22	89.53
2	63.15	5.06
3	34.56	2.77
4	10.20	0.82
5	7.97	0.64
6	4.07	0.33
7	3.73	0.30
8	2.42	0.19
9	1.31	0.10
10	0.94	0.08
11	0.74	0.06
12	0.54	0.04
13	0.48	0.04
14	0.25	0.02
15	0.23	0.02
16	0.06	0.00
17	0.00	0.00

Campylosphaera, *Helicosphaera*, and *Pontosphaera* are consistently very rare in lower Eocene samples with very slight increases in abundance (~1%) above ~250 crmcd in the middle Eocene.

Blackites is a minor component in the lower Eocene assemblages but displays a shift in abundance up to 3–4% near the base of Chron C21n.

PCA reveals that two significant principal components (PCA1, PCA2) account for 94.6% of the variance (Table 2). Factor 1 (PC1, 89.5% of the variance) is characterized by a high negative loading on *Reticulofenestra* (−0.8), whereas it is positively loaded on *Zygrhablithus* (0.50) and, to a lesser extent, on *Coccolithus* (0.15), *Sphenolithus* (0.12), and *Discoaster* (0.09). The loadings of the others species are considered too low to be significant. The trend of PC1 scores displays a gradual decrease along the section, marked by three negative shifts at ~268.45, 260.16, and 208.88 crmcd. Lower Eocene samples are characterized by positive values, whereas middle Eocene samples generally display negative values (Figure 3). Factor 2 (PC2, 5.06% of the variance) is strongly loaded by *Coccolithus* (−0.74) and *Zygrhablithus* (0.61). *Reticulofenestra* (0.22), *Dictyococcites* (0.15), and *Discoaster* (−0.09) are also considered significant. The PC2 trend shows a sharp increase between ~285 and ~279 crmcd (Figure 3).
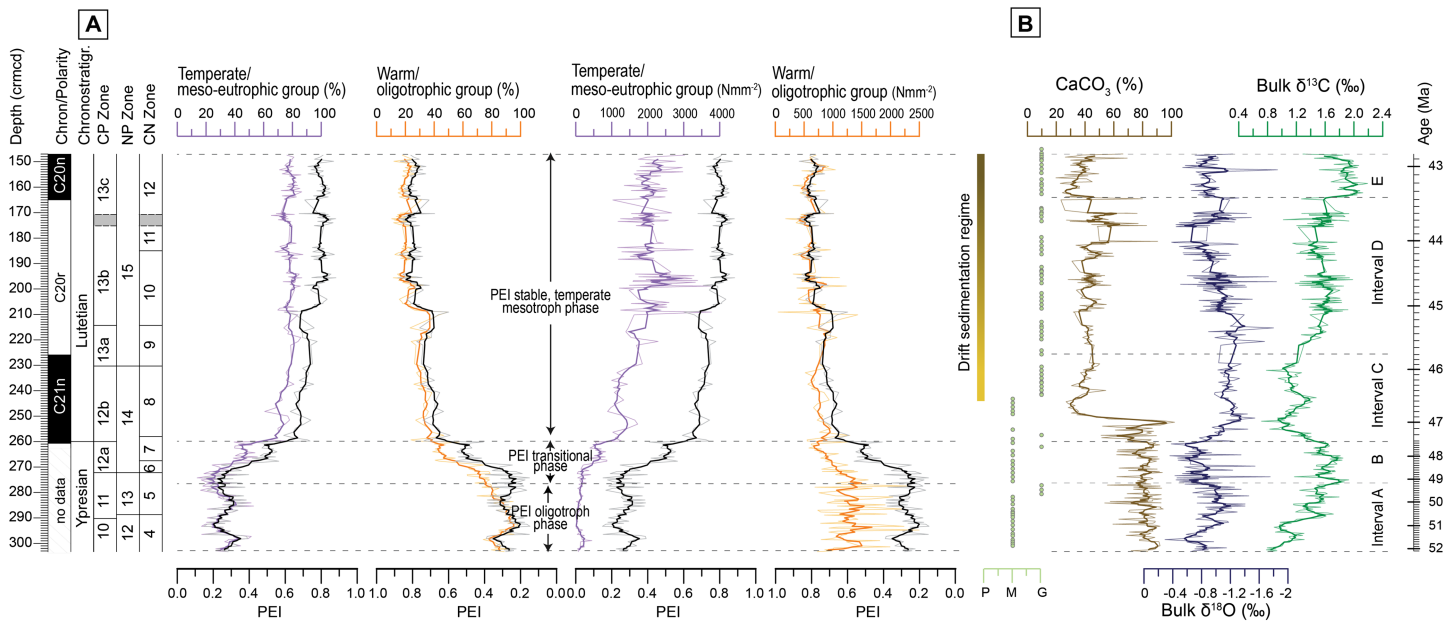
3.2. The PEI and the Long-Term Paleoecological Evolution

During the early to middle Eocene at Site U1410, the PEI indicates a significant change in the relative abundance of the temperate-water mesotrophic group and warm-water oligotrophic group (Figure 4a). From the base of the study interval at 303.29 crmcd up to 276.49 crmcd, the PEI shows broad fluctuations around a mean value of 0.35, reflecting the dominance of warm-water oligotrophs. Two transient increases (at ~291 and ~277 crmcd) in abundance of the warm-water/oligotrophic group are shaped by high abundances of one species, *Discoaster kuepperi*. From 276.49 crmcd up to 259.97 crmcd, the PEI progressively increases to 0.8, reflecting increases in the temperate-water/mesotrophic group (mainly *Reticulofenestra*) and decline of warm-water/oligotrophic taxa. The PEI remains high and constant through the middle Eocene with a mean value of 0.80 and a very low standard deviation (0.04). The stable and high PEI values in the middle

Figure 3. Results of the PCA obtained from relative abundances of selected calcareous nannofossil genera. To the left: distribution patterns of PC1, PC2 are plotted against chronostratigraphy, magnetostratigraphy, and calcareous nannofossil biostratigraphy: CP Zone (Okada & Bukry, 1980), NP Zone (Martini, 1971), and CNE Zone (Agnini et al., 2014). To the right: loading plots of the two principal components.

Figure 4. Site U1410 calcareous nannofossil PaleoEnvironmental Index (PEI) and geochemical data are plotted versus calcareous nannofossil biozonations (CP Zone, Okada & Bukry, 1980; NP Zone, Martini, 1971; and CNE Zone, Agnini et al., 2014) and magnetostratigraphy. The time scale to the right is calibrated to GTS12, and it is based on available chron boundaries and on the top of *Tribrachiatus orthostylus*. Darker lines are 5 point moving average data sets. (a) The calcareous nannofossil PaleoEnvironmental Index (PEI; black line) is presented against relative abundance (%) and semiquantitative abundance (N/mm^2) of nannofossil paleoecological groups (upper axis). Dotted lines highlight key intervals defined here based on PEI. (b) From left to right: calcareous nannofossil preservation estimate (P = poor; M = moderate; G = good; Norris et al., 2012), carbonate content (CaCO$_3$), and stable oxygen (δ^{18}O) and carbon (δ^{13}C) isotope records from bulk sediments. The vertical brown bar indicates the presence of a sediment drift regime. To the right, Intervals A–E represent the subdivision used here to describe stable isotope and carbonate content trends.

Eocene result from high abundances of temperate water/meso-eutrophic taxa and low abundances of the warm-water/oligotrophic group, which rarely exceed 20% of the assemblage.

3.3. Bulk Stable Isotope Data and CaCO$_3$ Content

The bulk carbonate carbon (δ^{13}C) and oxygen (δ^{18}O) stable isotopes records and carbonate content (CaCO$_3$) data show distinctive trends and several minor excursions that allow for a subdivision of the study section in five intervals (A–E; Figure 4b) based on isotopic patterns and lithologic changes.

3.3.1. Carbon Isotopes

Bulk carbon isotope values in the study section range between 0.71‰ and 2.19‰ with an average of 1.48‰ and a standard deviation (1σ) of ±0.31‰. From the base of the succession to 276.48 crmcd, we identify an interval (Interval A) where the δ^{13}C values have an average of 1.26‰ (±0.24‰). Superimposed on a long-term, upsection increasing trend, the δ^{13}C record shows several small negative CIEs with magnitudes ranging from 0.28‰ to 0.57‰ (Figure 4b). From 276.48 to 257.57 crmcd (Interval B), the δ^{13}C show relatively high values that average ~1.78‰ (±0.02‰ 1σ).

The third interval (Interval C: 251.52–224.132 crmcd, broadly corresponding to Chron C21n) is characterized by the lowest δ^{13}C values (1.13 ± 0.28‰ 1σ). The lower part of this interval (251.52–242.11 crmcd) is characterized by a distinctive negative shift with magnitude of 0.5‰. From 224.132 to 164.02 crmcd (Interval D), the bulk δ^{13}C record displays a trend toward higher values (1.55 ± 0.2‰ 1σ). Just above the base of Chron C20n (164.026 crmcd), the curve shows a second abrupt shift toward higher values (1.89 ± 0.18‰ 1σ; Interval E).

3.3.2. Oxygen Isotopes

Bulk oxygen isotope values in the study section vary between −0.29‰ and −1.88‰, with a mean value of −0.9‰ (±0.28‰ 1σ). In the lower part of the study section (Interval A), the δ^{18}O record is characterized by the highest mean values of the entire succession (−0.91‰). The δ^{18}O values sharply increase by ~0.2‰ between ~278 and ~276 crmcd in the interval that encompasses the base of Interval B (−0.77 ± 0.29‰ 1σ). At the base of Interval C, there is a negative δ^{18}O trend, with minimum δ^{18}O values of −1.54‰ at 244.76

crmcd (Figure 4b). Throughout Interval D, $\delta^{18}O$ values display a long-term increase with an average value of ~−1.05‰ (±0.30‰ 1σ). The general increase in $\delta^{18}O$ values is followed by a slight decrease in the uppermost part of Interval D. The base of Interval E is marked by a shift toward higher values and upward values that remains stable approximately −0.90‰ (Figure 4b).
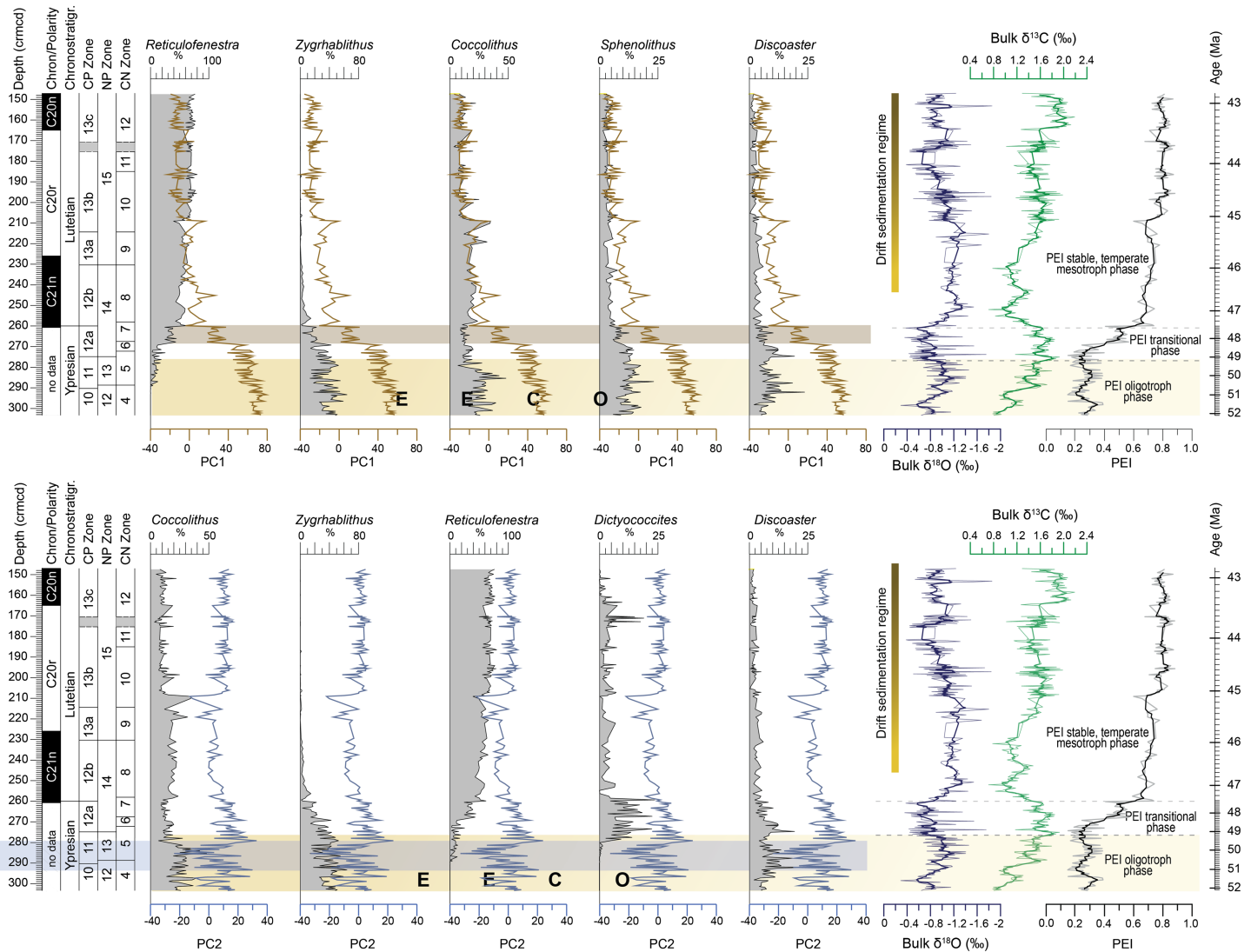
3.3.3. Carbonate Content

The lower ~46 m of the study succession (Intervals A and B) are characterized by high $CaCO_3$ content, varying between 50% and 100% and averaging 81%. The lower part of Interval C is characterized by a prominent and abrupt drop in the carbonate content by ~50% at ~251 crmcd. Above ~244.5 crmcd in the upper ~61 m of the study section, the carbonate content remains stable with a mean value of ~42% (±6.63% 1σ). At 181.62 crmcd, $CaCO_3$ concentration abruptly increases upsection from ~44% to 90%. Above this level and in the uppermost ~17 m, the %$CaCO_3$ shows several prominent peaks reaching values between 76% and 90%, with a mean value of ~53% (~±15% 1σ). A significant shift toward lower values is observed at the base of Interval E (~161 crmcd), where $CaCO_3$ content averages ~35% (Figure 4b).

4. Discussion

4.1. Major Changes in the Calcareous Nannofossil Record

The early to middle Eocene interval is a major turning point in Cenozoic calcareous nannofossil assemblage composition, shifting from a dominance of *Toweius* to reticulofenestrids (Agnini et al., 2006;Schneider et al., 2011 ; Shamrock & Watkins, 2012). This turnover is not only remarkable in terms of the magnitude of change in abundance of key taxa but also greatly impacted the long-term evolution of nannofossil assemblages. Indeed, the early to middle Eocene expansion of the reticulofenestrids represents the first step of this group's rise to current global dominance, as seen in the modern ocean with *Gephyrocapsa* and *Emiliana*. Site U1410 allows us to analyze the timing and significance of this major transition as well as the nature of the modifications observed in the nannofossil assemblages in the North Atlantic during the initial phase in the evolution of the reticulofenestrids. Studies on modern coccolithophore populations suggest that changes in assemblage composition are mainly controlled by the thermal and nutrient structure of surface waters (Gibbs et al., 2006; Okada & Honjo, 1973). In general, highly eutrophic environments favor lower diversity assemblages with abundant meso/eutrophic taxa that exploit high nutrient conditions. In contrast, stable and oligotrophic environments support lower abundance but higher diversity communities. Pioneering studies on the biogeography of Paleogene nannofossils have shown that numerous taxa displayed a clear preference for specific temperature and nutrient conditions (Aubry, 1992, 1998; Haq & Lohmann, 1976; Wei & Wise, 1990). Although the potential of nannofossils in paleoecological reconstructions has been largely recognized by the scientific community, there is still a degree of uncertainty especially when considering extinct taxa for which very little is known about their life strategies (Billard & Innouye, 2004; Young et al., 2005). In addition, the broader response of calcareous nannoplankton to surface water perturbations (Newsam et al., 2017) compared with other planktonic groups (e.g., foraminifera) and the uncertain signals displayed by some taxa in different paleoenvironments can hinder, at least in part, the application of nannofossils as paleoenviromental proxies (Bown & Pearson, 2009; Schneider et al., 2013; Villa et al., 2008). There is, however, a broad consensus regarding the environmental preferences of many Paleogene taxa, and calcareous nannoplankton still remain one of the most important tools for paleoclimatic/paleoceanographic reconstructions, given their ubiquitous and abundant occurrence in the marine sedimentary archive. At Site U1410 study section, the potential paleoenvironmental signal from calcareous nannofossil assemblages was investigated by using the PCA that allows to assess potential components that impacted calcareous nannofossil assemblages and to identify major loading taxa.

Most of the variance in nannofossil assemblages at Site U1410 is explained by PC1, which shows a pattern that is broadly mirrored by the abundance trend of *Reticulofenestra* and, to a lesser extent, of *Zygrhablithus* (Figure 5). Two abrupt negative shifts (at ~48.2 and ~47.4 Ma), which coincide with prominent increase in abundance of *Reticulofenestra*, punctuate the decreasing long-term trend of PC1. Following the second shift at ~47.4 Ma, the assemblage remains relatively constant, and a new "steady state" is reached for the rest of the study interval (to ~42.8 Ma), characterized by very high (mean value ~60%) percentages of *Reticulofenestra*. As *Reticulofenestra* reached stable, high abundances, the abundance of the holococcolith *Zygrhablithus* also declined significantly and never recovered to abundance levels observed in the early

Figure 5. Comparison of PC1, PC2 patterns with the relative abundance trends (%) of the strongest loading taxa, bulk stable isotope records, and PaleoEnvironmental Index. Light brown and light blue green bands highlight intervals in which principal components show significant variations. To the left, chronostratigraphy, magnetostratigraphy, and calcareous nannofossil biostratigraphy: CP Zone (Okada & Bukry, 1980), NP Zone (Martini, 1971), and CNE Zone (Agnini et al., 2014). The time scale to the right is calibrated to GTS12, and it is based on available chron boundaries and on the top of *Tribrachiatus orthostylus*.

Eocene. This pattern indicates that the latest Ypresian recorded an important change in calcareous nannofossil assemblages that permanently shaped their structure.

The decline of *Zygrhablithus* along with the increase of *Reticulofenestra* at the early to middle Eocene transition is a global signature that was previously observed at both middle and high latitudes (Schneider et al., 2011; Shamrock & Watkins, 2012). Although the interpretation of abundance of *Zygrhablithus* patterns is complicated by preservational influences (Bown et al., 2008; Jiang & Wise, 2009; Wind & Wise, 1978), it is unlikely that *Zygrhablithus* abundance at Site U1410 is significantly impacted by preservation. There is no evidence of systematic alteration, either in the lower Eocene nannofossil chalks, where early calcite overgrowth protects specimens of *Zygrhablithus*, or in the middle Eocene clay-rich sediments, where the effects of dissolution are considered to be minimal.

The PC1 loadings of nannofossil taxa at Site U1410 are coherent with their previous inferred paleoecological affinities (e.g., Bralower, 2002; Schneider et al., 2011; Wei & Wise, 1990), as loadings are positive for those taxa adapted to warm-oligotrophic conditions (*Zygrhablithus*, *Coccolithus*, *Discoaster*, and *Sphenolithus*) and negative for *Reticulofenestra*, which include temperate-water, mesotrophic taxa. The PC1 therefore is

likely correlated to temperature and to lesser extent to productivity/nutrient conditions. Indeed, the timing of the long-lasting shift in PC1 documented at Site U1410 at ~48.19 Ma suggests that this change is related to the global post-EECO cooling that begins at ~49 Ma (Westerhold et al., 2018).

The PC2 loadings highlight changes in assemblage composition that took place during the climax of the EECO (~51–49.5 Ma; Figure 5). Although this component accounts for only a small amount of the variance, it is noteworthy that a major shift in PC2 corresponds with the time of the *Toweius*-reticulofenestrid turnover, when these taxa display relatively low abundances. The PC2 is strongly negatively loaded by *Coccolithus* and positively loaded by *Zygrhablithus*, which are the two dominant assemblage components throughout the climax of EECO. During the major shift of PC2, *Coccolithus* shows a prominent drop, whereas *Zygrhablithus* remains relatively constant.

The trends of *Coccolithus* and *Zygrhablithus* observed at Site U1410 are similar to those reported from North Atlantic Gobar Spur sites by Schneider et al. (2011). These authors suggested that the global early expansion of *Reticulofenestra* is related to a progressive thermal destratification and a decrease in the oceanic biological pumping efficiency that initiated at high latitudes and culminated at ~51 Ma. At Site U1410, the observed decrease in the oligotrophic *Discoaster* and the concomitant early expansion of reticulofenestrids provide further support to this hypothesis. Fluctuations of the PC2 during EECO might therefore be indicative of changes in the trophic structure of surface waters related to an enhanced nutrient supply and increased vertical mixing. However, the interpretation of calcareous nannofossil changes during this interval is problematic because the ecological adaptations of the two main taxa controlling PC2 loadings (*Coccolithus* and *Zygrhablithus*) are not fully understood. Our data suggest that *Coccolithus* was hindered by the increased nutrient supply in the middle Eocene, whereas *Zygrhablithus* shows no response through the same interval, perhaps indicating a wider tolerance to changing trophic conditions.

4.2. Calcareous Nannofossil Assemblages and Paleoenvironmental Evolution

In the Site U1410 study section, the nannofossil PEI and stable isotope values show distinctive trends that allow us to explore relative timings of changes observed in the two records. Variations in bulk $\delta^{18}O$ and $\delta^{13}C$ reflect the stable isotope composition of a mixture of multiple carbonate components but are primarily a record derived from calcareous nannofossils, which typically form the largest component in marine pelagic carbonates. Changes in bulk isotope record may therefore be affected to some extent by changes in calcareous nannofossil assemblages due to different interspecific isotope fractionations (e.g., Hermoso et al., 2014, 2016; Ziveri et al., 2003). However, increasing lines of evidence indicate that changes observed in bulk $\delta^{13}C$ during the Eocene are global and reflect variations in the composition of the inorganic carbon pool (DIC) of the ocean, which in turn depends mainly on primary productivity, temperature, and CO_2 exchange with the atmosphere (Slotnick et al., 2012). The $\delta^{18}O$ record is a valid qualitative indicator for past changes in sea surface water temperatures during periods of limited continental glaciation, even though the $\delta^{18}O$ signal can be strongly affected by diagenetic alteration (Slotnick et al., 2015). As a note of caution, we are aware that the ooze/chalk interval (the EECO interval) has a lower preservation if compared with the upper interval and this might have affected the pristine bulk $\delta^{18}O$ record of Site U1410, at least partially.

Based on trends and changes observed in the PEI, our succession can be subdivided in three distinctive intervals: (1) the lower part of the succession where warm-water, oligotrophs prevail, (2) a middle part with transitional assemblages, and (3) the upper part where temperate mesotrophs dominate (Figure 4a).

4.2.1. The PEI Oligotroph Phase (~52.1 to 49.2 Ma)

In this earliest phase, the PEI indicates sustained warm-water and oligotrophic conditions. Fluctuations in the PEI are consistent with those observed in the stable isotope record, which shows relatively low $\delta^{18}O$ values with multiple short-term high amplitude fluctuations (Figures 4 and 5). Several transient negative excursions may relate to more widely recognized CIEs (Kirtland Turner et al., 2014; Luciani et al., 2016, 2017; Sexton et al., 2011; Slotnick et al., 2012; Slotnick et al., 2015; Slotnick, Lauretano, et al., 2015; Westerhold et al., 2017, 2018) that punctuate the long-term $\delta^{13}C$ trend. The interval is therefore characterized by variability of both the biotic and geochemical records, with the background warm-oligotrophic conditions intermittently interrupted by more temperate and eutrophic intervals.

Throughout this interval, major changes of calcareous nannofossil assemblages are also recorded by PC2, which has been shown to be related to changes in nutrient supply on the basis of the findings of

Schneider et al. (2011). The progressive change toward more productive and slightly cooler surface waters is also suggested by bulk δ^{13}C record. The PEI record is largely controlled by the abundance of discoasters (mainly *D. kuepperi*), which shows prominent fluctuations, while other warm taxa (e.g., *Sphenolithus* and *Zygrhablithus*) remain relatively stable or decrease (*Coccolithus*). Eutrophic groups, such as reticulofenestrids and *Toweius*, have somewhat discontinuous occurrences that represent either their onset or final occurrence, respectively.

4.2.2. The PEI Transitional Phase (~49.2 to 47.4 Ma)

In this interval, the PEI significantly increases as the warm, oligotrophs progressively decline and temperate, mesotrophs increase (Figure 4a). This trend reflects the major changes related to PC1, involving the decrease of *Zygrhablithus* (from >50% to <10%), the decrease of *Sphenolithus* and *Discoaster* (from ~15% to <10%), and the increase of *Reticulofenestra* to 50% (Figure 5).

The base of this interval is marked by a positive shift in bulk δ^{18}O and by a reversal in the trend of δ^{13}C (Figure 5). The small shift in bulk δ^{18}O (~0.2‰) corresponds to a clear increase in the PEI, which supports a link between changes in temperature and nannofossil community composition, as suggested by PC1. The high nannoplankton sensitivity to the environmental change is likely related to the fact that the background conditions of the EECO were probably close to a threshold which was exceeded, resulting in significant changes in assemblages. This is especially true for those taxa that were better adapted to the extreme warm and oligotrophic conditions. Small but prolonged changes in thermal structure might have affected these ecological niches, causing a contraction of the sensitive K-specialist communities and favoring an expansion of the more opportunist *Reticulofenestra*.

The switch from warm-oligotrophic to temperate meso-eutrophic assemblages is thus related to a global transition toward cooler conditions probably related to the post-EECO cooling, rather than directly connected to the paleoceanographic evolution of the study area. Indeed, at Site U1410, the dominance of reticulofenestrids (~50% of calcareous nannofossil assemblages) is reached at ~48.19 Ma, ~1 Ma before the prominent lithological change associated with the onset of the drift sedimentation.

4.2.3. The PEI Stable, Temperate Mesotroph Phase (~47.4 to 42.8 Ma)

Warm-water oligotrophs represent less than 20% of the assemblages by ~47.4 Ma (Figure 4a) and continued to slowly decline to 42.8 Ma, suggesting a gradual shift toward more temperate and eutrophic conditions. The stability observed in the PEI values is not reflected in abiotic proxies (Figure 5). Indeed, although a restoration of warmer conditions characterizes the lower middle Eocene intervals associated with negative stable isotope excursions, we document a persistent dominance of *Reticulofenestra* and any recovery of the warm-water oligotrophs. This trend is possibly explained if the environmental perturbations have not passed the threshold required to force significant modifications in the composition of nannofossil assemblages. This lower middle Eocene excursion interval in stable isotope records slightly precedes the significant drop in $CaCO_3$ content reflecting the initial formation of the Northern Component Water (Boyle et al., 2017; Coxall et al., 2018; Vahlenkamp et al., 2018).

The dominance of *Reticulofenestra* throughout the middle Eocene is a global signal, but changes in deep ocean circulation in the North Atlantic may have resulted in enhanced nutrient availability in sea surface waters triggering an amplification in dominance of reticulofenestrids at Site U1410.

Reticulofenestrids show a high degree of morphological variability, and there is no clear consensus on the generic-level taxonomy, with some authors applying one or two genera in the Eocene (*Reticulofenestra* and *Cyclicargolithus*, e.g., Bown & Dunkley Jones, 2012; Bown & Newsam, 2017; Newsam et al., 2017) and some applying two more (e.g., *Dictyococcites* and *Cribrocentrum*, e.g., Agnini et al., 2014; Fornaciari et al., 2010; Perch-Nielsen, 1985; Schneider et al., 2011; Tori & Monechi, 2013). At Site U1410, early reticulofenestrids mainly include small- to medium-sized elliptical forms with open central areas filled by very fragile or almost imperceptible nets (*Reticulofenestra*) and small- to medium-sized elliptical forms with a central area that is covered by a relatively developed plug (*Dictyococcites* spp. sensu, Fornaciari et al., 2010). *Reticulofenestra* and *Dictyococcites* both appeared at the *Toweius*-reticulofenestrids turnover, but, whereas *Reticulofenestra* expanded throughout the early to middle Eocene, *Dictyococcites* declined in the early stages of the PEI stable, temperate mesotroph phase at ~47.2 Ma. The different abundance patterns in *Reticulofenestra* and *Dictyococcites* are interpreted to reflect subtle differences in the optimum conditions for these taxa. Different ecological adaptations between *Dictyococcites* and *Reticulofenestra* have been first

pointed out by Schneider et al. (2011), suggesting that *Reticulofenestra* was characterized by a more mesotrophic ecology than *Dictyococcites*. We hypothesize that the progressive evolution toward more temperate and eutrophic conditions, as indicated by the PEI trends, likely led to the decline of more oligotrophic, warm-water favoring *Dictyococcites*, providing a competitive advantage to *Reticulofenestra*, which eventually dominates the assemblages of the middle Eocene.

The nannofossil assemblage data set developed in this study from Site U1410 documents the progressive development of a new structure in the middle Eocene calcareous nannofossil assemblages. The major switch from the early Eocene warm-oligotrophic communities to the middle Eocene temperate-eutrophic community occurred within a ~2-Myr time window spanning the end of EECO and the Ypresian-Lutetian boundary (~49.2 to 47.4 Ma). At Site U1410, the PEI transitional interval is coupled with a shift to relatively high bulk $\delta^{18}O$ values, suggesting that after the EECO, small magnitude long-lasting changes in sea surface temperatures were sufficient to favor one of the most important reconfiguration in the Cenozoic calcareous nannofossil assemblages.

5. Conclusions

Site U1410 on Southeast Newfoundland Ridge provides the first continuous sedimentary record in the North Atlantic basin across the early to middle Eocene transition. Sedimentation at this site is marked by a prominent change to drift sedimentation across the early to middle Eocene transition controlled by northern-sourced deep waters. We document calcareous nannofossil assemblage evolution over a ~9-Myr interval (~52.1 to 42.8 Ma), spanning the end of the EECO to the early phase of middle Eocene global cooling.

Nannofossil assemblage data from Site U1410 reveal a major shift from the early to middle Eocene, characterized by the gradual increase of *Reticulofenestra* and progressive decline of *Toweius*, *Zygrhablithus*, *Discoaster*, and *Sphenolithus* that dominate in the EECO assemblages. We suggest that this permanent and profound rearrangement of calcareous nannofossil assemblages is the result of the major paleoenvironmental changes occurred in the early to middle Eocene. During the EECO, the first fundamental step in the evolution of assemblages, the *Toweius*-reticulofenestrids turnover, took place. This long-lasting shift in the main components of the assemblages was associated to significant paleoenvironmental instability, as suggested by the trend of the stable isotope records and of the PEI, which mainly reflects abundance fluctuations in *Discoaster*. Our findings further support the hypothesis that the early expansion of *Reticulofenestra* during the EECO was favored by the establishment of more unstable and eutrophic conditions, probably driven by a progressive thermal destratification (Schneider et al., 2011).

The second and larger step in the nannofossil assemblages is marked by a notable increase in abundance of *Reticulofenestra* and permanent decline of warm-water oligotrophs (*Zygrhablithus*, *Discoaster*, *Sphenolithus*) during the PEI transitional phase (~49.2 to 47.4 Ma). The onset of this phase coincides with a positive shift in bulk $\delta^{18}O$ record, interpreted to indicate post-EECO cooling that reduced the optimal habitat space for oligotrophs and favored the expansion of the cosmopolitan *Reticulofenestra*.

In the youngest part of our study interval, middle Eocene nannofossil assemblages are dominated by *Reticulofenestra*, but the stable isotope records indicate a transient reversal in the long-term cooling trend. This may relate to a transient warming episode close the early/middle Eocene boundary (Intxauspe-Zubiaurre et al., 2017; Intxauspe-Zubiaurre et al., 2017; Payros et al., 2012; Westerhold et al., 2018), but its identification and correlation worldwide remains problematic. In fact, it is becoming increasingly clear that climate and carbon cycle dynamics during the initial phase of the post-EECO long-term cooling might have been more complicated than originally thought, and further data sets are thus required to better constrain this crucial time interval.

References

Agnini, C., Fornaciari, E., Raffi, I., Catanzariti, R., Pälike, H., Backman, J., & Rio, D. (2014). Biozonation and biochronology of Paleogene calcareous nannofossils from low and middle latitudes. *Newsletters on Stratigraphy*, *47*, 131–181. http://doi.org/10.1127/0078-0421/2014/0042

Agnini, C., Fornaciari, E., Rio, D., Tateo, F., Backman, J., & Giusberti, L. (2007). Responses of calcareous nannofossil assemblages, mineralogy and geochemistry to the environmental perturbations across the Paleocene/Eocene boundary in the Venetian Pre-Alps. *Marine Micropaleontology*, *63*, 19–38. http://doi.org/10.1016/j.marmicro.2006.10.002

Agnini, C., Monechi, S., & Raffi, I. (2017). Calcareous nannofossil biostratigraphy: Historical background and application in Cenozoic chronostratigraphy. *Lethaia*, *50*, 447–463. http://doi.org/10.1111/let.12218

Agnini, C., Muttoni, G., Kent, D. V., & Rio, D. (2006). Eocene biostratigraphy and magnetic stratigraphy from Possagno, Italy: The calcareous nannofossil response to climate variability. *Earth and Planetary Science Letters*, *241*, 815–830. http://doi.org/10.1016/j.epsl.2005.11.005

Agnini, C., Spofforth, D. J. A., Dickens, G. R., Rio, D., Pälike, H., Backman, J., et al. (2016). Stable isotope and calcareous nannofossil assemblage record of the late Paleocene and early Eocene (Cicogna Section). *Climate of the Past*, *12*, 883–909. http://doi.org/10.5194/cp-12-883-2016

Anagnostou, E., John, E. H., Edgar, K. M., Foster, G. L., Ridgwell, A., Inglis, G. N., et al. (2016). Changing atmospheric CO_2 concentration was the primary driver of early Cenozoic climate. *Nature*, *533*(7603), 380–384. http://doi.org/10.1038/nature17423

Applegate, J. L., & Wise Jr., S. W. (1987). Eocene calcareous nannofossils, Deep Sea Drilling Project Site 605, upper continental rise off New Jersey U.S.A. Initial Reports of the Deep Sea Drilling Project (vol. 93, pp. 685-698). Washington: U.S. Govt. Printing Office.

Aubry, M.-P. (1984). *Handbook of Cenozoic calcareous nannoplankton, book 1, Ortholithae (Discoaster)*. New York: American Museum of Natural History Micropaleontology Press.

Aubry, M.-P. (1989). *Handbook of Cenozoic calcareous nannoplankton, book 3, Ortholithae (Pentaliths and other), Heliolithae (Fasciculiths, Sphenoliths and others)*. New York: American Museum of Natural History Micropaleontology Press.

Aubry, M.-P. (1992). Late Paleogene calcareous nannoplankton evolution: A tale of climatic deterioration. In D. R. Prothero, & W. A. Berggren (Eds.), *Eocene-Oligocene climatic and biotic evolution*, (pp. 272–309). Princeton: Princeton University Press.

Aubry, M.-P. (1998). Early Paleogene calcareous nannoplankton evolution: A tale of climatic amelioration. In M.-P. Aubry, S. G. Lucas, & W. A. Berggren (Eds.), *Late Paleocene–early Eocene biotic and climatic events in the marine and terrestrial records*, (pp. 158–201). New York: Columbia University Press.

Backman, J. (1986). Late Paleocene to middle Eocene calcareous nannofossil biochronology from the Shatsky Rise, Walvis Ridge and Italy. *Palaeogeography, Palaeoclimatology, Palaeoecology*, *57*, 43–59. http://doi.org/10.1016/0031-0182(86)90005-2

Backman, J., & Hermelin, J. O. R. (1986). Morphometry of the Eocene nannofossil *Reticulofenestra umbilicus* lineage and its biochronological consequences. *Palaeogeography, Palaeoclimatology, Palaeoecology*, *57*, 103–116. https://doi.org/10.1016/0031-0182(86)90009-X

Backman, J., Raffi, I., Rio, D., Fornaciari, E., & Pälike, H. (2012). Biozonation and biochronology of Miocene through Pleistocene calcareous nannofossils from low and middle latitudes. *Newsletters on Stratigraphy*, *45*(3), 221–244. http://doi.org/10.1127/0078-0421/2012/0022

Backman, J., & Shackleton, N. J. (1983). Quantitative biochronology of Pliocene and early Pleistocene calcareous nannofossils from the Atlantic, Indian and Pacific oceans. *Marine Micropaleontology*, *8*, 141–170. https://doi.org/10.1016/0377-8398(83)90009-9

Beerling, D. J., & Royer, D. L. (2011). Convergent Cenozoic CO_2 history. *Nature Geoscience*, *4*, 418–420. http://doi.org/10.1038/ngeo1186

Berggren, W. A., & Aubry, M.-P. (1984). Rb-Sr glauconite isochron of the Eocene Castle Hayne Limestone, North Carolina: Further discussion. *Geological Society of America Bulletin*, *95*(3), 364–370.

Bernaola, G., Orue-Etxebarria, X., Payros, A., Dinarès-Turell, J., Tosquella, J., Apellaniz, E., & Caballero, F. (2006). Biomagnetostratigraphic analysis of the Gorrondatxe section (Basque Country, Western Pyrenees): Its significance for the definition of the Ypresian/Lutetian boundary stratotype. *Neues Jahrbuch Fur Geologie Und Palaontologie – Abhandlungen*, *241*, 67–109.

Bijl, P. K., Bendle, J. A. P., Bohaty, S. M., Pross, J., Schouten, S., Tauxe, L., et al. (2013). Eocene cooling linked to early flow across the Tasmanian Gateway. *Proceedings of the National Academy of Sciences of the United States of America*, *110*(24), 9645–9650. https://doi.org/10.1073/pnas.1220872110

Bijl, P. K., Schouten, S., Sluijs, A., Reichart, G. J., Zachos, J. C., & Brinkhuis, H. (2009). Early Palaeogene temperature evolution of the southwest Pacific Ocean. *Nature*, *461*(7265), 776–779. https://doi.org/10.1038/nature08399

Billard, C., & Innouye, I. (2004). What is new in coccolithophore biology? In H. R. Thierstein, & J. R. Young (Eds.), *Coccolithophores: From molecular processes to global impact*, (Vol. 1, pp. 1–29). New York: Springer-Verlag Berlin Heidlberg. https://doi.org/10.1007/978-3-662-06278-4

Bohaty, S. M., & Zachos, J. C. (2003). Significant Southern Ocean warming event in the late middle Eocene. *Geology*, *31*(11), 1017–1020. https://doi.org/10.1130/G19800.1

Bohaty, S. M., Zachos, J. C., Florindo, F., & Delaney, M. L. (2009). Coupled greenhouse warming and deep-sea acidification in the middle Eocene. *Paleoceanography*, *24*, PA2207. https://doi.org/10.1029/2008PA001676

Boulila, S., Vahlenkamp, M., de Vleeschouwer, D., Laskar, J., Yamamoto, Y., Pälike, H., et al. (2018). Towards a robust and consistent middle Eocene astronomical timescale. *Earth and Planetary Science Letters*, *486*, 94–107. https://doi.org/10.1016/j.epsl.2018.01.003

Bown, P. R. (2005). Palaeogene calcareous nannofossils from the Kilwa and Lindi areas of coastal Tanzania (Tanzania Drilling Project 2003-4). *Journal of Nannoplankton Research*, *27*(1), 21–95.

Bown, P. R., & Dunkley Jones, T. (2006). New Paleogene calcareous nannofossil taxa from coastal Tanzania: Tanzania Drilling Project Sites 11 to 14. *Journal of Nannoplankton Research*, *28*(1), 17–34.

Bown, P. R., & Dunkley Jones, T. (2012). Calcareous nannofossils from the Paleogene equatorial Pacific (IODP Expedition 320 Sites U1331-1334). *Journal of Nannoplankton Research*, *32*(2), 3–51.

Bown, P. R., Dunkley Jones, T., Lees, J. A., Randell, R. D., Mizzi, J. A., Pearson, P. N., et al. (2008). A Paleogene calcareous microfossil Konservat-Lagerstätte from the Kilwa Group of coastal Tanzania. *Bulletin of the Geological Society of America*, *120*(1-2), 3–12. https://doi.org/10.1130/B26261.1

Bown, P. R., & Newsam, C. (2017). Calcareous nannofossils from the Eocene North Atlantic Ocean (IODP Expedition 342 Sites U1403–1411). *Journal of Nannoplankton Research*, *37*(1), 25–60.

Bown, P. R., & Pearson, P. (2009). Calcareous plankton evolution and the Paleocene-Eocene thermal maximum event: New evidence from Tanzania. *Marine Micropaleontology*, *71*, 60–70. https://doi.org/10.1016/j.marmicro.2009.01.005

Bown, P. R., & Young, J. R. (1998). Techniques. In P. R. Bown (Ed.), *Calcareous nannofossil biostratigraphy*, (pp. 16–28). Cambridge: Kluwer Academic Publishers.

Boyle, P. R., Romans, B. W., Tucholke, B. E., Norris, R. D., Swift, S. A., & Sexton, P. F. (2017). Cenozoic North Atlantic deep circulation history recorded in contourite drifts, offshore Newfoundland, Canada. *Marine Geology*, *385*, 185–203. https://doi.org/https://doi.org/10.1016/j.margeo.2016.12.014

Bralower, T. J. (2002). Evidence of surface water oligotrophy during the Paleocene-Eocene Thermal Maximum: Nannofossil assemblage data from Ocean Drilling Program Site 690, Maud Rise, Weddell Sea. *Paleoceanography*, *17*(2), PA1023. https://doi.org/10.1029/2001PA000662

Bukry, D. (1973). Low-latitude coccolith biostratigraphic zonation. In N. T. Edgar, J. B. Saunders, et al. (Eds.), *Initial reports DSDP 15*, (pp. 685–703). Washington: U. S. Govt. Printing Office. http://doi.org/10.2973/dsdp.proc.15.116.1973

Coplen, T. B., Brand, W. A., Gehre, M., Gröning, M., Meijer, H. J., Toman, B., & Verkouteren, R. M. (2006). New guidelines for $\delta^{13}C$ measurements. *Analytical Chemistry*, *78*(7), 2439–2441. http://doi.org/10.1021/ac052027c

Coxall, H. K., Huck, C. E., Huber, M., Lear, C. H., Legarda-Lisarri, A., O'Regan, M., et al. (2018). Export of nutrient rich Northern Component Water preceded early Oligocene Antarctic glaciation. *Nature Geoscience*, *11*(3), 190–196. http://doi.org/10.1038/s41561-018-0069-9

Coxall, H. K., & Pearson, P. N. (2007). The Eocene-Oligocene Transition. In M. Williams, A. Hayward, J. Gregory, & D. N. Schmidt (Eds.), *Deep-time perspectives on climate change: Marrying the signal from computer models and biological proxies*, (pp. 351–387). London: The Geological Society.

Cramer, B. S., Wright, J. D., Kent, D. V., & Aubry, M.-P. (2003). Orbital climate forcing of $\delta^{13}C$ excursions in the late Paleocene-early Eocene (Chrons C24n-C25n). *Paleoceanography*, *18*(4), PA1097. https://doi.org/10.1029/2003PA000909

Cramwinckel, M. J., Huber, M., Kocken, I. J., Agnini, C., Bijl, P. K., Bohaty, S. M., et al. (2018). Synchronous tropical and polar temperature evolution in the Eocene. *Nature*, *559*(7714), 382–386. http://doi.org/10.1038/s41586-018-0272-2

Dallanave, E., Agnini, C., Muttoni, G., & Rio, D. (2009). Magneto-biostratigraphy of the Cicogna section (Italy): Implications for the late Paleocene-early Eocene time scale. *Earth and Planetary Science Letters*, *285*, 39–51. http://doi.org/10.1016/j.epsl.2009.05.033

Dickens, G. R. (2011). Down the Rabbit Hole: Toward appropriate discussion of methane release from gas hydrate systems during the Paleocene-Eocene Thermal Maximum and other past hyperthermal events. *Climate of the Past*, *7*, 831–846. https://doi.org/10.5194/cp-7-831-2011

Drury, A. J., Westerhold, T., Hodell, D., & Röhl, U. (2018). Reinforcing the North Atlantic backbone: Revision and extension of the composite splice at ODP Site 982. *Climate of the Past*, *14*, 321–338. http://doi.org/10.5194/cp-14-321-2018

Dunkley Jones, T., Bown, P. R., Pearson, P. N., Wade, B. S., Coxall, H. K., & Lear, C. H. (2008). Major shifts in calcareous phytoplankton assemblages through the Eocene-Oligocene Transition of Tanzania and their implications for low-latitude primary production. *Paleoceanography*, *23*, PA4204. https://doi.org/10.1029/2008PA001640

Erbacher, J., Mosher, D. C., Malone, M. J. & Shipboard Scientific Party (2004). Demerara Rise: Equatorial Cretaceous and Paleogene Paleoceanographic Transect, Western Atlantic. Proceedings of the ocean drilling program, initial reports, 207. College Station, TX: Ocean Drilling Program. http://doi.org/10.2973/odp.proc.ir.207.2004

Fornaciari, E., Agnini, C., Catanzariti, R., Rio, D., Bolla, E. M., & Valvasoni, E. (2010). Mid-latitude calcareous nannofossil biostratigraphy and biochronology across the middle to late Eocene transition. *Stratigraphy*, *7*, 229–264.

Gibbs, S. J., Bralower, T. J., Bown, P. R., Zachos, J. C., & Bybell, L. M. (2006). Shelf and open-ocean calcareous phytoplankton assemblages across the Paleocene-Eocene Thermal Maximum: Implications for global productivity gradients. *Geology*, *34*(4), 233–236. http://doi.org/10.1130/G22381.1

Greenwood, D. R., & Wing, S. L. (1995). Eocene continental climates and latitudinal temperature gradients. *Geology*, *23*, 1044–1048. http://doi.org/10.1130/0091-7613(1995)023<1044:ECCALT>2.3.CO;2

Hammer, Ø., Harper, D. A. T., & Ryan, P. D. (2011). PAST: Paleontological statistics software package for education and data analysis. *Palaeontologia Electronica*, *4-9*.

Haq, B. U., & Lohmann, G. P. (1976). Early Cenozoic calcareous nannoplankton biogeography of the Atlantic Ocean. *Marine Micropaleontology*, *1*, 119–194. http://doi.org/10.1016/0377-8398(76)90008-6

Hermoso, M., Chan, I. Z. X., McClelland, H. L. O., Heureux, A. M. C., & Rickaby, R. E. M. (2016). Vanishing coccolith vital effects with alleviated carbon limitation. *Biogeosciences*, *13*, 301–3012. http://doi.org/10.5194/bg-13-301-2016

Hermoso, M., Horner, T. J., Minoletti, F., & Rickaby, R. E. M. (2014). Constraints on the vital effect in coccolithopore and dinoflagellate calcite by oxygen isotopic modification of seawater. *Geochimica et Cosmochimica Acta*, *141*, 612–627.

Hollis, C. J., Handley, L., Crouch, E. M., Morgans, H. E. G., Baker, J. A., Creech, J., et al. (2009). Tropical sea temperatures in the high-latitude South Pacific. *Geology*, *37*(2), 99–102. http://doi.org/10.1130/G25200A.1

Hollis, C. J., Taylor, K. W. R., Handley, L., Pancost, R. D., Huber, M., Creech, J. B., et al. (2012). Early Paleogene temperature history of the Southwest Pacific Ocean: Reconciling proxies and models. *Earth and Planetary Science Letters*, *349-350*, 53–66. http://doi.org/10.1016/j.epsl.2012.06.024

Hull, P. M., et al. (2017). Data report: Coarse fraction record for the Eocene megas-plice at IODP Sites U1406, U1408, U1409, and U1411. Proceedings of the Integrated Ocean Drilling Program, 342. College Station, TX: Integrated Ocean Drilling Program.

Intxauspe-Zubiaurre, B., Flores, J., & Payros, A. (2017). Variations to calcareous nannofossil $CaCO_3$ content during the middle Eocene C21r-H6 hyperthermal event (~47.4 Ma) in the Gorrondatxe section (Bay of Biscay, Western Pyrenees). *Palaeogeography, Palaeoclimatology, Palaeoecology*, *487*, 296–306. http://doi.org/10.1016/j.palaeo.2017.09.015

Intxauspe-Zubiaurre, B., Payros, A., Flores, J., & Apellaniz, E. (2017). Changes to sea-surface characteristics during the middle Eocene (47.4 Ma) C21r-H6 event: Evidence from calcareous nannofossil assemblages of the Gorrondatxe section (Western Pyrenees). *Newsletters on Stratigraphy*, *50*, 245–267. http://doi.org/10.1127/nos/2017/0305

Jiang, S., & Wise, S. W. Jr. (2009). Distinguishing the influence of diagenesis on the paleoecological reconstruction of nannoplankton across the Paleocene/Eocene Thermal Maximum: An example from the Kerguelen Plateau, southern Indian Ocean. *Marine Micropaleontology*, *72*, 49–59. http://doi.org/10.1016/j.marmicro.2009.03.003

Kennett, J. P. (1977). Cenozoic evolution of Antarctic glaciation, the Circum-Antarctic Ocean, and their impact on global paleoceanography. *Journal of Geophysical Research*, *82*, 3843–3860. https://doi.org/10.1029/JC082i027p03843

Kirtland Turner, S., Sexton, P. F., Charles, C. D., & Norris, R. D. (2014). Persistence of carbon release events through the peak of early Eocene global warmth. *Nature Geoscience*, *7*, 748–751. http://doi.org/10.1038/NGEO2240

Luciani, V., Dickens, R. G., Backman, J., Fornaciari, E., Giusberti, L., Agnini, C., & D'Onofrio, R. (2016). Major perturbations in the global carbon cycle and photosymbiont-bearing planktic foraminifera during the early Eocene. *Climate of the Past*, *12*, 981–1007. http://doi.org/10.5194/cp-12-981-2016

Luciani, V., D'Onofrio, R., Dickens, G. R., & Wade, B. S. (2017). Planktic foraminiferal response to Early Eocene carbon cycle perturbations in the Southeast Atlantic Ocean (ODP Site 1263). *Global and Planetary Change*, *158*, 119–133. http://doi.org/10.1016/j.gloplacha.2017.09.007

Lunt, D. J., Ridgwell, A., Sluijs, A., Zachos, J., Hunter, S., & Haywood, A. (2011). A model for orbital pacing of methane hydrate destabilization during the Palaeogene. *Nature Geoscience*, *4*(11), 775–778. http://doi.org/10.1038/ngeo1266

Martini, E. (1971). Standard Tertiary and Quaternary calcareous nannoplankton zonation. In A. Farinacci (Ed.), *Proceedings 2nd International Conference Planktonic Microfossils Roma*, (pp. 739–785). Roma: Tecnoscienza.

Martini, E., & Müller, C. (1986). Current Tertiary and Quaternary calcareous nannoplankton stratigraphy and correlations. *Newsletters on Stratigraphy*, *16*, 99–112. http://doi.org/10.1127/nos/16/1986/99

Molina, E., Alegret, L., Apellaniz, E., Bernaola, G., Caballero, F., Dinarès-Turell, J., et al. (2011). The Global Stratotype Section and Point (GSSP) for the base of the Lutetian Stage at the Gorrondatxe section, Spain. *Episodes*, *34*(2), 86–108. https://doi.org/10.18814/epiiugs/2011/v34i2/006

Monechi, S., Buccianti, A., & Gardin, S. (2000). Biotic signals from nannoflora across the iridium anomaly in the upper Eocene of the Massignano section: Evidence from statistical analysis. *Marine Micropaleontology*, *39*, 219–237. http://doi.org/10.1016/S0377-8398(00)00022-0

Muttoni, G., & Kent, D. V. (2007). Widespread formation of cherts during the early Eocene climate optimum. *Palaeogeography, Palaeoclimatology, Palaeoecology*, *253*, 348–362. http://doi.org/10.1016/j.palaeo.2007.06.008

Newsam, C., Bown, P. R., Wade, B. S., & Jones, H. L. (2017). Muted calcareous nannoplankton response at the Middle/Late Eocene Turnover Event in the Western North Atlantic Ocean. *Newsletters on Stratigraphy*, *50*(3), 297–309. http://doi.org/10.1127/nos/2016/030

Norris, R. D., Expedition 342 Scientists (2012). Paleogene Newfoundland sediment drifts. Integrated Ocean Drilling Program Expedition 342 Preliminary Report. College Station, TX: Integrated Ocean Drilling Program Management International, Inc., for the Integrated Ocean Drilling Program. http://doi.org/10.2204/iodp.pr.342.2012

Norris, R. D., Klaus, A., & Kroon, D. (2001). Mid-Eocene deep water, the Late Palaeocene Thermal Maximum and continental slope mass wasting during the Cretaceous-Palaeogene impact. *Geological Society, London, Special Publications*, *183*(1), 23–48. http://doi.org/10.1144/GSL.SP.2001.183.01.02

Norris, R. D., Kroon, D., Huber, B. T., & Erbacher, J. (2001). Cretaceous-Palaeogene ocean and climate change in the subtropical North Atlantic. *Geological Society, London, Special Publications*, *183*(1), 1–22. http://doi.org/10.1144/GSL.SP.2001.183.01.01

Norris, R. D., Wilson, P. A., Blum, P., & Expedition 342 Scientists (2014). *Paleogene Newfoundland sediment drifts and MDHS test. Proceedings of the Integrated Ocean Drilling Program*, (Vol. 342). College Station, TX: Integrated Ocean Drilling Program. http://doi.org/10.2204/iodp.proc.342.2014

Okada, H., & Bukry, D. (1980). Supplementary modification and introduction of code numbers to the low-latitude coccolith biostratigraphic zonation (Bukry, 1973; 1975). *Marine Micropaleontology*, *5*, 321–325. http://doi.org/10.1016/0377-8398(80)90

Okada, H., & Honjo, S. (1973). The distribution of oceanic coccolithophorids in the Pacific. *Deep-Sea Research and Oceanographic Abstracts*, *20*, 355–364, IN3-IN4,365-374. http://doi.org/10.1016/0011-7471(73)90059-4

Pagani, M., Zachos, J. C., Freeman, K. H., Tipple, B., & Bohaty, S. M. (2005). Atmospheric science: Marked decline in atmospheric carbon dioxide concentrations during the Paleogene. *Science*, *309*(5734), 600–603. http://doi.org/10.1126/science.1110063

Payros, A., Ortiz, S., Alegret, L., Orue-Etxebarria, X., Apellaniz, E., & Molina, E. (2012). An early Lutetian carbon-cycle perturbation: Insights from the Gorrondatxe section (western Pyrenees, Bay of Biscay). *Paleoceanography*, *27*, PA2213. https://doi.org/10.1029/2012PA002300

Perch-Nielsen, K. (1985). Cenozoic calcareous nannofossils. In H. M. Bolli, J. B. Saunders, & K. Perch-Nielsen (Eds.), *Plankton stratigraphy*, (pp. 427–554). Cambridge University Press: Cambridge.

Persico, D., & Villa, G. (2004). Eocene-Oligocene calcareous nannofossils from Maud Rise and Kerguelen Plateau (Antarctica): Paleoecological and paleoceanographic implications. *Marine Micropaleontology*, *52*, 153–179. http://doi.org/10.1016/j.marmicro.2004.05.002

Raffi, I. (1999). Precision and accuracy of nannofossil biostratigraphic correlation. *Philosophical Transactions of the Royal Society A: Mathematical, Physical and Engineering Sciences*, *357*, 1975–1993. http://doi.org/10.1098/rsta.1999.0410

Schneider, L. J., Bralower, T. J., & Kump, L. R. (2011). Response of nannoplankton to early Eocene ocean destratification. *Palaeogeography, Palaeoclimatology, Palaeoecology*, *310*, 152–162. http://doi.org/10.1016/j.palaeo.2011.06.018

Schneider, L. J., Bralower, T. J., Kump, L. R., & Patzkowsky, M. E. (2013). Calcareous nannoplankton ecology and community change across the Paleocene-Eocene Thermal Maximum. *Paleobiology*, *39*, 628–647.

Self-Trail, J. M., Seefelt, E. L., Sheperd, C. L., & Martin, V. A. (2017). Biostratigraphic and morphometric analyses of specimens from calcareous nannofossil genus *Tribrachiatus*. *Journal of Nannoplankton Research*, *37*(2-3), 177–188.

Sexton, P. F., Norris, R. D., Wilson, P. A., Pälike, H., Westerhold, T., Röhl, U., et al. (2011). Eocene global warming events driven by ventilation of oceanic dissolved organic carbon. *Nature*, *471*(7338), 349–352. http://doi.org/10.1038/nature09826

Shamrock, J. L., & Watkins, D. K. (2012). Eocene calcareous nannofossil biostratigraphy and community structure from Exmouth Plateau, Eastern Indian Ocean (ODP Site 762). *Stratigraphy*, *9*, 1–54.

Slotnick, B. S., Dickens, G. R., Hollis, C. J., Crampton, J. S., Percy Strong, C., & Phillips, A. (2015). The onset of the Early Eocene Climatic Optimum at Branch Stream, Clarence River valley, New Zealand. *New Zealand Journal of Geology and Geophysics*, *58*, 262–280. http://doi.org/10.1080/00288306.2015.1063514

Slotnick, B. S., Dickens, G. R., Nicolo, M. J., Hollis, C. J., Crampton, J. S., Zachos, J. C., & Sluijs, A. (2012). Large-amplitude variations in carbon cycling and terrestrial weathering during the latest Paleocene and earliest Eocene: The record at Mead Stream, New Zealand. *Journal of Geology*, *120*, 487–505. http://doi.org/10.1086/666743

Slotnick, B. S., Lauretano, V., Backman, J., Dickens, G. R., Sluijs, A., & Lourens, L. (2015). Early Paleogene variations in the calcite compensation depth: New constraints using old borehole sediments from across Ninetyeast Ridge, Central Indian Ocean. *Climate of the Past*, *11*, 473–493. http://doi.org/10.5194/cp-11-473-201

Spofforth, D. J. A., Agnini, C., Pälike, H., Rio, D., Fornaciari, E., Giusberti, L., et al. (2010). Organic carbon burial following the Middle Eocene Climatic Optimum in the central western Tethys. *Paleoceanography*, *25*, PA3210. https://doi.org/10.1029/2009PA001738

Toffanin, F., Agnini, C., Fornaciari, E., Rio, D., Giusberti, L., Luciani, V., et al. (2011). Changes in calcareous nannofossil assemblages during the Middle Eocene Climatic Optimum: Clues from the central-western Tethys (Alano section, NE Italy). *Marine Micropaleontology*, *81*(1-2), 22–31. http://doi.org/10.1016/j.marmicro.2011.07.002

Tori, F., & Monechi, S. (2013). Lutetian calcareous nannofossil events in the Agost section (Spain): Implications toward a revision of the middle Eocene biomagnetostratigraphy. *Lethaia*, *46*, 293–307. https://doi.org/10.1111/let.12008

Tremolada, F., & Bralower, T. J. (2004). Nannofossil assemblage fluctuations during the Paleocene-Eocene Thermal Maximum at Sites 213 (Indian Ocean) and 401 (North Atlantic Ocean): Palaeoceanographic implications. *Marine Micropaleontology*, *52*, 107–116. http://doi.org/10.1016/j.marmicro.2004.04.002

Vahlenkamp, M., Niezgodzki, I., De Vleeschouwer, D., Bickert, T., Harper, D., Kirtland Turner, S., et al. (2018). Astronomically paced changes in deep-water circulation in the western North Atlantic during the middle Eocene. *Earth and Planetary Science Letters*, *484*, 329–340. http://doi.org/10.1016/j.epsl.2017.12.016

Vandenberghe, N., Hilgen, F. J., & Speijer, R. P. (2012). The Paleogene period. In F. M. Gradstein, J. C. Ogg, M. D. Schmitz, & G. M. Ogg (Eds.), *The geological timescale 2012*, (pp. 855–922). Amsterdam: Elsevier. http://doi.org/10.1016/B978-0-444-59425-9.00028-7

Villa, G., Fioroni, C., Pea, L., Bohaty, S. M., & Persico, D. (2008). Middle Eocene-late Oligocene climate variability: Calcareous nannofossil response at Kerguelen Plateau, Site 748. *Marine Micropaleontology*, *69*, 173–192. http://doi.org/10.1016/j.marmicro.2008.07.00

Villa, G., Fioroni, C., Persico, D., Roberts, A. P., & Florindo, F. (2014). Middle Eocene to late Oligocene Antarctic glaciation/deglaciation and Southern Ocean productivity. *Paleoceanography*, *29*, 223–237. https://doi.org/10.1002/2013PA002518

Wei, W., & Wise, S. W. Jr. (1989). Paleogene calcareous nannofossil magnetobiochronology: Results from South Atlantic DSDP Site 516. *Marine Micropaleontology*, *14*, 119–152. http://doi.org//10.1016/0377-8398(89)90034-0

Wei, W., & Wise, S. W. Jr. (1990). Biogeographic gradients of middle Eocene-Oligocene calcareous nannoplankton in the South Atlantic Ocean. *Palaeogeography, Palaeoclimatology, Palaeoecology*, *79*, 29–61. http://doi.org/10.1016/0031-0182(90)90104-F

Westerhold, T., Röhl, U., Donner, B., & Zachos, J. C. (2018). Global extent of early Eocene hyperthermal events: A new Pacific benthic foraminiferal isotope record from Shatsky Rise (ODP Site 1209). *Paleoceanography and Paleoclimatology*, *33*, 626–642. http://doi.org/10.1029/2017PA003306

Westerhold, T., Röhl, U., Frederichs, T., Agnini, C., Raffi, I., Zachos, J. C., & Wilkens, R. H. (2017). Astronomical calibration of the Ypresian timescale: Implications for seafloor spreading rates and the chaotic behavior of the solar system? *Climate of the Past*, *13*, 1129–1152. http://doi.org/10.5194/cp-13-1129-201

Wilkens, R. H., Westerhold, T., Drury, A. J., Lyle, M., Gorgas, T., & Tian, J. (2017). Revisiting the Ceara Rise, equatorial Atlantic Ocean: Isotope stratigraphy of ODP Leg 154 from 0 to 5 Ma. *Climate of the Past*, *13*, 779–793. https://doi.org/10.5194/cp-13-779-2017

Wind, F. H., & Wise, S. W. (1978). Mesozoic holococcoliths. *Geology*, *6*(3), 140–142. http://doi.org/10.1130/0091-7613(1978)6<140:MH>2.0.CO;2

Yamamoto, Y., Fukami, H., Taniguchi, W., & Lippert, P. C. (2018). Data report: Updated magnetostratigraphy for IODP Sites U1403, U1408, U1409, and U1410. Proceedings of the Integrated Ocean Drilling Program, 342. College Station, TX: Integrated Ocean Drilling Program. http://doi.org/10.2204/iodp.proc.342.207.2018 2

Young, J. R., Geisen, M., & Probert, I. (2005). A review of selected aspects of coccolithophore biology with implications for paleobiodiversity estimation. *Micropaleontology*, *51*(4), 267–288. http://doi.org/10.2113/gsmicropal.51.4.267

Zachos, J., Pagani, H., Sloan, L., Thomas, E., & Billups, K. (2001). Trends, rhythms, and aberrations in global climate 65 Ma to present. *Science*, *292*(5517), 686–693. http://doi.org/10.1126/science.1059412

Zachos, J. C., Dickens, G. R., & Zeebe, R. E. (2008). An early Cenozoic perspective on greenhouse warming and carbon cycle dynamics. *Nature*, *451*(7176), 279–283. http://doi.org/10.1038/nature06588

Ziveri, P., Stoll, H., Probert, I., Klaas, C., Geisen, M., Ganssen, G., & Young, J. (2003). Stable isotope 'vital effects' in coccolith calcite. *Earth and Planetary Science Letters*, *210*, 137–149. http://doi.org/10.1016/S0012-821X(03)00101-8